$^1O_2$ Generation

DOI: 10.1002/anie.201105236

Metal Nanoparticles Sensitize the Formation of Singlet Oxygen**

*Raviraj Vankayala, Arunachalam Sagadevan, Priya Vijayaraghavan, Chien-Lin Kuo, and Kuo Chu Hwang**

Singlet oxygen ($^1O_2$) is known to play an indispensible role in the photodynamic therapy (PDT) treatment of cancer,[1–5] and is an important oxidant for hydroperoxidation of olefins in organic synthesis.[6,7] Singlet O_2 is conventionally formed by sensitization by organic photosensitizers, such as Rose Bengal, silicon phthalocyanine, etc.[1–7] These organic or organometallic dyes are, however, prone to photoinduced degradation and enzymatic degradation, which becomes problematic in PDT treatments, and reduces the efficiency of the generation of singlet O_2.[5,8] It is, therefore, important to search for photosensitizers with highly efficient singlet O_2 generation and large absorption coefficients that are photochemically more stable and less prone to enzymatic degradation.

Previously, it was reported that the yield of singlet oxygen production by a photosensitizer, namely, Rose Bengal, was enhanced by a silver island film through the metal-enhanced absorption of photosensitizer.[9,10] It was also reported that a gold nanodisk could enhance the phosphorescence decay rate of singlet oxygen, leading to a larger characteristic phosphorescence emission band of singlet oxygen at 1270 nm.[11] In another two studies, it was observed that the quantum yield of singlet O_2 formation generated by phthalocyanine photosensitizers can be enhanced by the presence of gold nanoparticles.[12,13] Herein we report an unprecedented observation that singlet oxygen can be formed through direct sensitization by metal nanoparticles (M NPs, M = Ag, Pt, and Au) without the presence of any organic photosensitizers. Unambiguous experimental evidence includes direct observation of singlet oxygen emission at roughly 1268 nm, hydroperoxidation of cyclohexene, green fluorescence from a selective singlet oxygen fluorescent sensor, namely, Singlet Oxygen Sensor Green (SOSG, Molecular Probe), and quenching of singlet oxygen phosphorescence by sodium azide.

As shown in Figure 1, photoexcitation of M NPs at the surface plasmon resonance absorption bands of Ag ($d = 55$, 42 nm), Pt (10 nm), and Au (22 nm) in D_2O results in characteristic singlet oxygen emission at 1264 and 1268 nm, respectively. Control experiments show that in the absence of metal nanoparticles, photoexcitation of poly(vinyl pyrrolidone (PVP) in D_2O using either 254 or 508 nm light did not result in any detectable singlet O_2 emission signal (see the

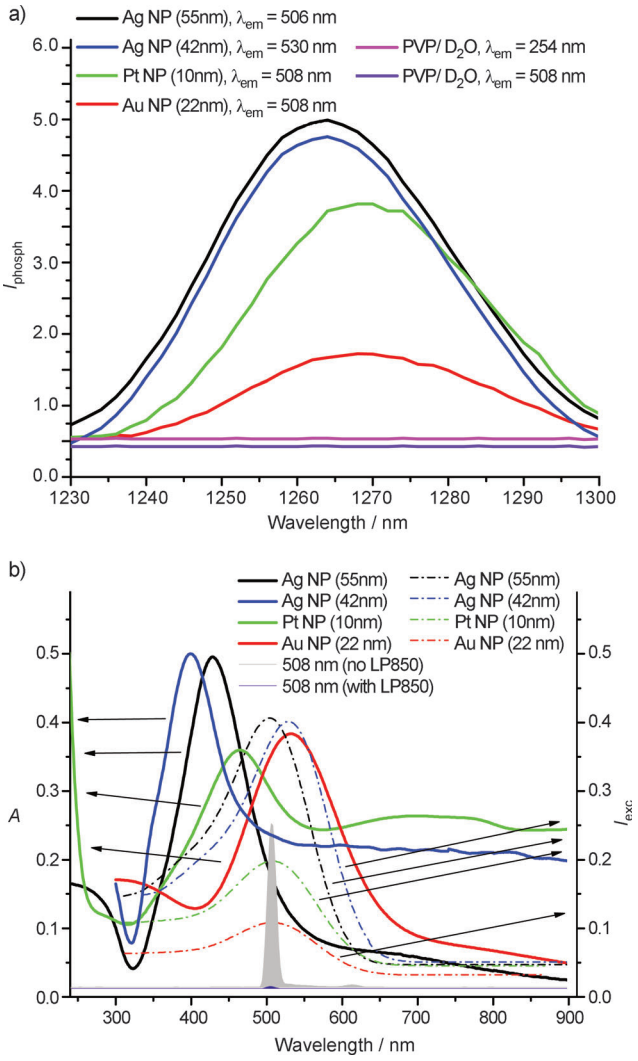

Figure 1. a) Phosphorescence emission spectra of singlet oxygen sensitized by Au, Ag or Pt nanoparticles in D_2O, and a control experiment with PVP in D_2O in the absence of metal nanoparticles (purple line, $\lambda_{ex} = 254$ nm and blue line, $\lambda_{ex} = 508$ nm). b) The extinction spectra (solid lines) of Ag, Pt, and Au NPs, and the excitation spectra (dashed lines) of singlet O_2 phosphorescence at 1270 nm in the presence of Ag, Pt, and Au NPs, respectively. A longpass filter of 850 nm was put between the sample and the detector for all experiments (unless otherwise mentioned) to filter away any stray light and the second harmonic of the excitation light with wavelengths shorter than 850 nm. The excitation light profiles of 508 nm are also shown (the gray blue line was recorded without the LP850 filter).

[*] R. Vankayala, A. Sagadevan, P. Vijayaraghavan, C.-L. Kuo, Prof. K. C. Hwang
Department of Chemistry, National Tsing Hua University
Hsinchu, Taiwan (R.O.C.)
E-mail: kchwang@mx.nthu.edu.tw

[**] We thank the National Science Council, Taiwan, for financial support.

Supporting information for this article is available on the WWW under http://dx.doi.org/10.1002/anie.201105236.

pink and purple lines in Figure 1 a). The control experiments clearly ruled out the possibility of the singlet O_2 emission signal being from stray light, scattered light, or an O_2–water charge-transfer complex.[14] Thus photoexcitation of Ag, Pt, and Au NPs in H_2O can result in the formation of singlet O_2. Replacement of PVP by hexadecylcetyltrimethyl ammonium bromide (CTAB) or trisodium citrate can also lead to the formation of singlet O_2. Sodium azide is known to be a very efficient electron-transfer quencher of singlet oxygen.[15] Control experiments also show that the singlet O_2 phosphorescence intensity becomes lower at higher concentrations of sodium azide (see Figure S1 in the Supporting Information).

All four M NPs have one major localized surface plasmon resonance (LSPR) band around 398–530 nm (see solid lines in Figure 1 b). The maximum of the excitation spectrum (see dashed lines in Figure 1 b) shifts from 504 to 529 nm when the size of the Ag NPs decreases from 55 to 42 nm. The excitation spectra show that excitation at wavelengths longer than 660 nm leads to negligible amount of singlet O_2 formation for all metal nanoparticles. Comparison of the LSPR of metal nanoparticles and the excitation spectra of singlet oxygen emission (see Figure 1 b) shows that the low-energy surface states of the metal nanoparticles can transfer energy to molecular oxygen with high efficiency and sensitize the formation of singlet oxygen (vide infra), whereas the high-energy surface states of M NPs transfer LSPR energy to molecular oxygen with low efficiencies. The mismatch between the excitation spectra and the absorption spectra indicates that metal nanoparticles, similar to azulene and their derivatives,[16] do not follow Kasha's rule,[17] and their plasmonically excited state behavior is strongly dependent on the excitation wavelengths. Such a result is attributed to the fact that the absorption/extinction spectrum of a metal nanoparticle is composed of many nonconjugated and localized surface plasmon resonances of different crystalline facets, and the LSPR of each metal nanoparticle behaves independently.

As shown in Figure 2, photoirradiation of cyclohexene in dichloromethane–acetonitrile in the presence of metal nanoparticles, such as Ag NPs ($d \approx 55$ nm), Au NPs (≈ 22 nm), and Pt NPs (≈ 10 nm), results in the formation of 2-hydroperoxyl cyclohexene (see Figure 2 a). The hydroperoxidation of cyclohexene to form 2-hydroperoxyl cyclohexene is known to occur in the presence of singlet oxygen.[18–20] In the ^{1}H NMR spectrum the observation of signals for an allylic proton at $\delta =$ 4.49 ppm, two vinyl protons ($\delta = 6.0$ and 5.74 ppm, multiplet), and a peroxide protons at $\delta = 8.5$ ppm indicate the formation of hydroperoxyl cyclohexene.[18–20] In the case of Au NPs, the peroxide signal at $\delta = 8.5$ ppm was absent, because of H–D exchange with the D_2O added to the solution to help disperse the nanoparticles. Formation of hydroperoxyl cyclohexene unambiguously supports the formation of singlet O_2 upon photoirradiation of M NPs. From the integration of the ^{1}H NMR spectra of the hydroperoxyl cyclohexene product (relative to an internal standard, 1,4-dicyanobenzene), it is clear that Ag NPs are more efficient than Pt and Au NPs at sensitizing the formation of singlet oxygen.

To further confirm that M NPs can indeed sensitize the formation of singlet O_2 upon photoirradiation, we used the

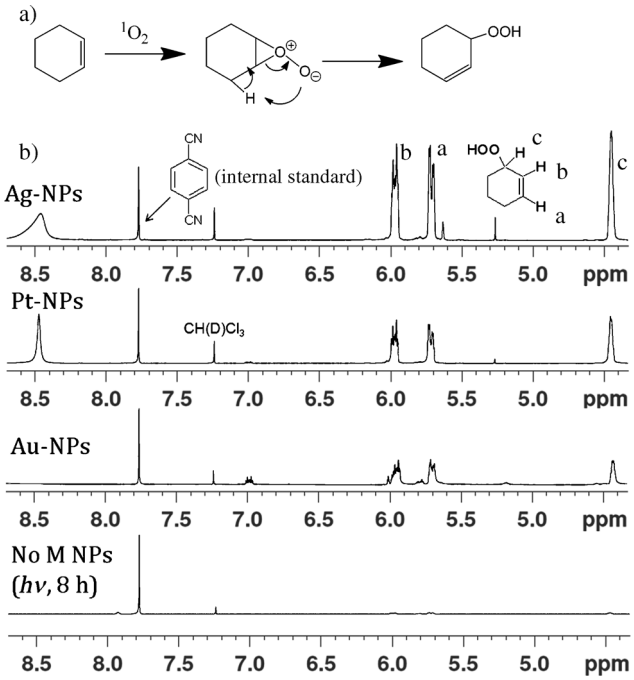

Figure 2. a) Reaction scheme of cyclohexene with singlet oxygen. b) ^{1}H NMR spectra of the photoinduced peroxidation product of cyclohexene in dichloromethane–acetonitrile (100 W high-pressure Hg lamp) in the presence of Ag NPs, Pt NPs, Au NPs, or in the absence of metal NPs. The signals of the peroxidation product, 2-hydroperoxyl cyclohexene, are assigned. In the case of Au NPs, a small amount of D_2O was added to help disperse the nanoparticles; this led D–H exchange of the R-OOH proton.

commercial singlet oxygen sensor SOSG to trap singlet O_2.[21,22] The chemical structure of SOSG was not disclosed, but it is believed to be an anthracene–fluorescein derivative.[21] SOSG has been demonstrated to have a very good selectivity towards singlet oxygen, and does not show any noticeable response towards hydroxyl radicals or superoxide.[22,23] Upon reaction with singlet O_2 to form endoperoxide, SOSG shows green fluorescence with an emission maximum at 525 nm. As shown in Figure 3, photoirradiation of metal NPs, including Ag, Pt, and Au NPs in D_2O in the presence of SOSG for 2 min results in the formation of strongly fluorescent SOSG ($\lambda_{em} = 525$ nm). The results clearly indicate that photoirradiation of metal nanoparticles indeed can result in the formation of singlet oxygen. In a control experiment, SOSG alone was irradiated in D_2O in the absence of metal nanoparticles; green fluorescence was observed, but with far weaker intensity (see the black line in Figure 3). The inset pictures in Figure 3 show the relative brightness of SOSG fluorescence in the presence of different M NPs. Our data (Figure 3) show that the amount of singlet O_2 formed through the sensitization of SOSG is negligible compared to the amounts of singlet O_2 formed through sensitization by M NPs. Overall, the results in Figures 1–3 all point to the conclusion that photoirradiation of metal nanoparticles in solution can indeed sensitize the formation of singlet oxygen.

To estimate the quantum yield of singlet O_2 formed through sensitization by metal nanoparticles, we used Rose

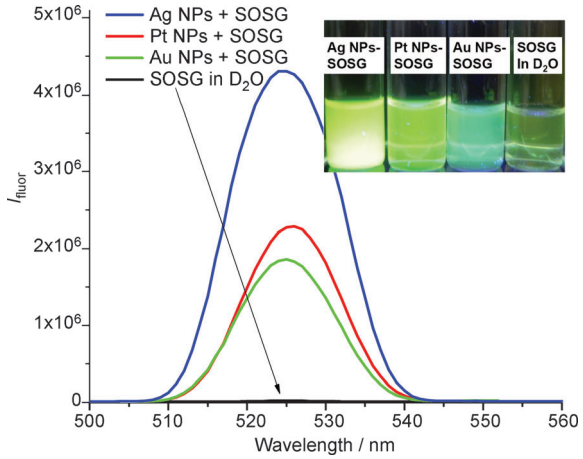

Figure 3. Fluorescence spectra of SOSG in D_2O in the presence of Ag NPs, Pt NPs, or Au NPs or in the absence of any metal NPs. The solutions were irradiated with a 100 W high-pressure Hg lamp for 2 min; excitation wavelength 382 nm. The inset shows green fluorescence emission from SOSG in four different D_2O solutions in the presence and absence of metal nanoparticles.

Bengal as a reference and calculated the singlet O_2 formation yields of different M NPs by comparing the phosphorescence emission area of singlet O_2 (integration area from 1225 to 1300 nm) with that obtained using Rose Bengal as a photosensitizer. Phosphorescence emission area, $Area_{phos,RB}$ is the product of the absorbance of Rose Bengal at 510 nm ($Ab_{RB\text{-}510}$), incident light intensity at 510 nm from the luminescence spectrometer, and the yield of singlet O_2 formation (Φ_{RB}) [Eq. (1)]. An analogous equation can be derived for metal nanoparticles [Eq. (2)].

$$Area_{phos\text{-}RB} = Ab_{RB\text{-}510} \times I_{510} \times \Phi_{RB} \quad (1)$$

$$Area_{phos\text{-}Ag} = Ab_{Ag\text{-}510} \times I_{510} \times \Phi_{Ag} \quad (2)$$

Rose Bengal is a commonly used singlet O_2 photosensitizer with a sensitization quantum yield of 0.76.[24] By taking the ratio of the phosphorescence area of singlet O_2, one obtains the singlet O_2 formation yields for M NPs to be 0.155, 0.085, and 0.037 for Ag, Pt, and Au NPs, respectively. Although M NPs have low singlet O_2 formation yields, they are still far better singlet O_2 photosensitizers than conventional organic dyes for the following reasons: 1) M NPs are far more resistant to photoinduced degradation and enzymatic degradation than organic dyes; 2) Metal nanoparticles have extinction coefficients 4–6 orders of magnitude higher than common organic dyes.[25,26] Our measurements (see Figure S2 in the Supporting Information) show that the extinction coefficients are 9.7×10^9 (at 531 nm), 2.5×10^9 (at 428 nm), 2.0×10^9 (at 399 nm), and $4.2\times10^6\,M^{-1}cm^{-1}$(at 463 nm) for Au NPs (22 nm), Ag NPs (55 nm), Ag NPs (44 nm) and Pt NPs (10 nm), respectively. These extinction coefficients are indeed 2–5 orders of magnitude higher that the extinction coefficients of Rose Bengal ($24\,335\,M^{-1}cm^{-1}$ at 514.5 nm).[27] The exceptionally high extinction coefficient of M NPs can easily compensate their slightly low singlet O_2 formation yields. Therefore, metal nanoparticles are expected to be far better photosensitizers than conventional organic dyes as PDT reagents for the production of singlet oxygen to kill cancer cells.

It was reported that the relaxation time to LSPR of metal nanoparticles is in the range of 10 fs to a few ps.[28,29] Such a short relaxation time will not allow energy transfer to occur by dynamic quenching, since the diffusion-limited rate ($\approx10^{10}\,M^{-1}s^{-1}$) of molecules in solution is far lower than the plasmon relaxation rate. So far, there is only one report in the literature describing energy transfer from plasmonically excited states of gold nanoparticles to surface-anchored phthalocyanines in 2.4 ps,[30] but there are many examples of fluorescence resonance energy transfer (FRET) from surface-bound chromophores to metal nanoparticles.[31–34] To have energy transfer occur from LSPR of M NPs to molecular oxygen (and thus formation of singlet O_2), molecular O_2 must be adsorbed on the surface of metal NPs. Low-energy electron diffraction (LEED) studies on metal single-crystal surfaces have shown that molecular O_2 can indeed be adsorbed on the surfaces of various metals, including, Au, Ag, and Pt,[35–37] which makes rapid energy transfer from LSPR to O_2 possible. Since the singlet O_2 was generated on the surface of metal nanoparticles, there might be some interactions between metal nanoparticles and singlet O_2, such as, metal-induced quenching or metal-enhanced phosphorescence.

It has been reported that many nanomaterials, upon photoexcitation, are able to sensitize the formation of singlet O_2. These nanomaterials include semiconductor quantum dots (QDs),[38,39] ZnO,[40,41] TiO_2,[42] and fullerenes.[43,44] Among the drawbacks for using semiconductor QDs as singlet O_2 photosensitizers are 1) the cytotoxicity of the cadmium ions, 2) the requirement of UV light for photoexcitation of QDs, and 3) the low quantum efficiency (≈0.05) of singlet O_2 sensitization.[38,39] The drawbacks for using ZnO as a singlet O_2 photosensitizer are its cytotoxicity ($IC_{50}=$ 49 ppm to human skin fibroblasts)[40] and low quantum yield for singlet O_2 generation.[41] The drawback of using TiO_2 nanoparticles to sensitize formation of singlet O_2 is its extremely poor absorption in the visible and near-IR region. In the case of fullerenes, the drawbacks include their insolubility in water, ready aggregation, and propensity to undergo photobleaching. Although the surface of fullerenes can be functionalized to improve the water solubility, it is at the expense of decreasing the quantum yield of singlet O_2 generation.[43] In addition, fullerenes contain many C=C bonds and are singlet O_2 quenchers. The weak absorption of fullerenes in the red or near-IR region is also one of their drawbacks as singlet O_2 photosensitizers.[44] The advantages of using metal nanoparticles as singlet O_2 photosensitizers are the following: 1) extinction coefficients 3–5 orders of magnitude higher than those of most other organic molecules and inorganic nanomaterials, 2) low cytotoxicity, especially for gold nanoparticles, and 3) tunability of light absorption wavelengths to the red or even near-IR region for large metal nanoparticles

In summary, we have reported an unprecedented observation that plasmonical excitation of metal nanoparticles,

including Au, Ag, and Pt NPs, leads to sensitization and formation of singlet oxygen. Direct evidence include the observation of phosphorescence emission of singlet O_2 at approximately 1268 nm, hydroperoxidation of olefins, fluorescence of a selective singlet oxygen sensor, and the quenching of singlet O_2 phosphorescence with sodium azide. We also demonstrate that similar to azulene and its derivatives, metal nanoparticles having many nonconjugated and localized surface plasmon resonance subdomains do not follow Kasha's rule; that is, their surface plasmonical photochemistry is strongly dependent on the excitation wavelengths. With their superior photostability, resistance to enzymatic degradation, and ultrahigh extinction coefficient (4–6 orders of magnitude higher those of than conventional organic dyes),[25,26] metal nanoparticles are expected to be far better singlet O_2 photosensitizers than conventional organic dyes for applications such as photodynamic therapy and the photoinduced peroxidation of olefins.

Experimental Section

The metal nanoparticles (Au, Ag, and Pt NPs) were prepared according to literature procedures,[45] and their structures and sizes determined by transmission electron microscopy (TEM, Jeol JEM-2100F, 200 KV) (see Figure S3 a–d in the Supporting Information for TEM images). Metal nanoparticles were dispersed in D_2O using a small amount of poly(vinyl pyrrolidone) (PVP, Aldrich, MW = 55000 g mol^{-1}). The phosphorescence emission of singlet O_2 was recorded using a luminescence spectrometer (FLS920, Edinburgh, equipped with a 450 W broadband Xe lamp) with a 850 nm longpass filter (Isuzu Optics, LP850) located in between the sample and detector to cut off any stray light and scattered light with wavelengths shorter than 850 nm. The output light intensities of the 450 W Xe lamp at 254 and 508 nm (with a slit width of 10 nm, values determined inside the sample chamber of the Edinburgh FLS920) are 1.5 and 2.5 mW, respectively. Hydroperoxidation of cyclohexene was conducted by photoirradiation of a solution containing 1 mL of cyclohexene and 1 mg of metal nanoparticles (M NPs, M = Au, Ag, and Pt) in dichloromethane (2 mL) and acetonitrile (4 mL). The M NPs were dispersed in the solution using PVP. The light source was a 100 W high-pressure Hg lamp without any filter, and the irradiation time was 8 h. The power densities on the sample solutions were 106 mW cm^{-2} at 410 nm, 28 mW cm^{-2} at 500 nm, 28 mW cm^{-2} at 532 nm, 17 mW cm^{-2} at 664 nm, and 14 mW cm^{-2} at 900 nm. After irradiation, the solvent and the starting material (cyclohexene) were removed by a rotatory evaporator at room temperature, and the residue was dissolved in $CDCl_3$ for ^{1}H NMR analysis (Varian, 400 MHz). Equal amounts of 1,4-dicyanobenzene were added to all samples to serve as an internal standard. All solvents and cyclohexene were purified according to literature procedures.[46]

In the singlet oxygen sensing experiments, stock solutions of fluorescent Singlet Oxygen Sensor Green (SOSG, Molecular Probe) were prepared by dissolving 100 μg of SOSG in methanol (33 μL) to make final concentration of approximately 5 mM. From the stock solution, 0.1 mM of SOSG was added into D_2O solution containing metal nanoparticles. The solution was then irradiated for 2 min using a 100 W high-pressure Hg lamp. Then the fluorescence emission of the coupling product of SOSG and singlet O_2 was recorded at 525 nm using an excitation light of 382 nm. In the generation of singlet O_2 by a dark reaction,[47] H_2O_2 (final concentration, 5 M) was added into an acetonitrile/water (50 v/v %) solution at pH 10.0 (adjusted with NaOH), followed by vigorous stirring for 1 min before measurement of singlet O_2 phosphorescence. Time-dependent phosphorescence intensity measurements show that the intensity of singlet O_2 phosphorescence remains quite constant during the first 8 min (decrease by roughly 3% 8 min after the mixing of H_2O_2 and acetonitrile).

Received: July 26, 2011
Published online: September 20, 2011

Keywords: energy transfer · metal-enhanced fluorescence · oxygen · nanoparticles · photochemistry

[1] P. R. Ogilby, *Chem. Soc. Rev.* **2010**, *39*, 3181.
[2] J. F. Lovell, T. W. B. Liu, J. Chen, G. Zheng, *Chem. Rev.* **2010**, *110*, 2839.
[3] D. E. J. G. J. Dolmans, D. Fukumura, R. K. Jain, *Nat. Rev. Cancer* **2003**, *3*, 380.
[4] N. Soh, *Anal. Bioanal. Chem.* **2006**, *386*, 532.
[5] M. C. DeRosa, R. J. Crutchley, *Coord. Chem. Rev.* **2002**, *233–234*, 351.
[6] M. N. Alberti, M. Orfanopoulos, *Tetrahedron* **2006**, *62*, 10660.
[7] E. L. Clennan, *Tetrahedron* **2000**, *56*, 9151.
[8] C. A. Kendall, C. A. Morton, *Technol. Cancer Res. Treat.* **2003**, *2*, 283.
[9] Y. Zhang, K. Aslan, M. J. R. Previte, C. D. Geddes, *J. Fluoresc.* **2007**, *17*, 345.
[10] Y. Zhang, K. Aslan, M. J. R. Previte, C. D. Geddes, *Proc. Natl. Acad. Sci. USA* **2008**, *105*, 1798.
[11] R. Toftegaard, J. Arnbjerg, K. Daasbjerg, P. R. Ogilby, A. Dmitriev, D. S. Sutherland, L. Poulsen, *Angew. Chem.* **2008**, *120*, 6114; *Angew. Chem. Int. Ed.* **2008**, *47*, 6025.
[12] D. C. Hone, P. I. Walker, R. Evans-Gowing, S. FitzGerald, A. Beeby, I. Chambrier, M. J. Cook, D. A. Russell, *Langmuir* **2002**, *18*, 2985.
[13] V. P. Chauke, E. Antunes, W. Chidawanyika, T. Nyokong, *J. Mol. Catal. A* **2011**, *335*, 121.
[14] R. D. Scurlock, P. R. Ogilby, *J. Phys. Chem.* **1989**, *93*, 5493.
[15] E. A. Lissi, M. V. Encinas, E. Lemp, M. A. Rubiot, *Chem. Rev.* **1993**, *93*, 699.
[16] G. Binsch, E. Hexibronner, R. Jankow, D. Schmidt, *Chem. Phys. Lett.* **1967**, *1*, 135.
[17] P. Klán, J. Wirz, *Photochemistry of Organic Compounds: From Concepts to Practice*, Wiley-Blackwell, Oxford, **2009**, p. 40.
[18] X. Xue, Y. Xu, *J. Mol. Catal. A* **2007**, *276*, 80.
[19] P. A. Burns, C. S. Foote, *J. Org. Chem.* **1976**, *41*, 908.
[20] A. Fukuoka, K. Fujishima, M. Chiba, A. Yamagishi, S. Inagaki, Y. Fukushimac, M. Ichikawa, *Catal. Lett.* **2000**, *68*, 241.
[21] X. Ragàs, A. Jiménez-Banzo, D. Sánchez-García, X. Batllori, S. Nonell, *Chem. Commun.* **2009**, 2920.
[22] C. Flors, M. J. Fryer, J. Waring, B. Reeder, U. Bechtold, P. M. Mullineaux, S. Nonell, M. T. Wilson, N. R. Baker, *J. Exp. Bot.* **2006**, *57*, 1725.
[23] Molecular Probe product information, **2004**.
[24] J. J. M. Lamberts, D. R. Schumacher, D. C. Neckers, *J. Am. Chem. Soc.* **1984**, *106*, 5879.
[25] P. K. Jain, K. S. Lee, I. H. El-Sayed, M. A. El-Sayed, *J. Phys. Chem. B* **2006**, *110*, 7238.
[26] K. Urbanska, B. Romanowska-Dixon, Z. Matuszak, J. Oszajca, P. Nowak-Sliwinska, G. Stochel, *Acta Biochim. Pol.* **2002**, *43*, 387.
[27] H. Du, R. A. Fuh, J. Li, A. Corkan, J. S. Lindsey, *Photochem. Photobiol.* **1998**, *68*, 141.
[28] M. Scharte, R. Porath, T. Ohms, M. Aeschlimann, J. R. Krenn, H. Ditlbacher, F. R. Aussenegg, A. Liebsch, *Appl. Phys. B* **2001**, *73*, 305.
[29] C. Burda, X. Chen, R. Narayanan, M. A. El-Sayed, *Chem. Rev.* **2005**, *105*, 1025.

[30] A. Kotiaho, R. Lahtinen, A. Efimov, H.-K. Metsberg, E. Sariola, H. Lehtivuori, N. V. Tkachenko, H. Lemmetyinen, *J. Phys. Chem. C* **2010**, *114*, 162.
[31] H. Chen, T. Ming, L. Zhao, F. Wang, L.-D. Sun, J. Wang, C.-H. Yan, *Nano Today* **2010**, *5*, 494.
[32] P. V. Kamat, *J. Phys. Chem. B* **2002**, *106*, 7729.
[33] T. K. Sau, A. L. Rogach, F. Jäckel, T. A. Klar, J. Feldmann, *Adv. Mater.* **2010**, *22*, 1805.
[34] K. E. Sapsford, L. Berti, I. L. Medintz, *Angew. Chem.* **2006**, *118*, 4676; *Angew. Chem. Int. Ed.* **2006**, *45*, 4562.
[35] H. Shi, C. Stampfl, *Phys. Rev. B* **2008**, *77*, 094127.
[36] L. Vattuone, M. Rocca, C. Boragno, U. Valbusa, *J. Chem. Phys.* **1994**, *101*, 713.
[37] C. T. Rettner, C. B. Mullins, *J. Chem. Phys.* **1991**, *94*, 1626.
[38] T. Nann, *Nano Biomed. Eng.* **2011**, *3*, 137.
[39] A. C. S. Samia, X. Chen, C. Burda, *J. Am. Chem. Soc.* **2003**, *125*, 15736.
[40] F. Dechsakulthorn, A. Hayes, S. Bakand, L. Joeng, C. Winder, *Proc. 6th World Congress on Alternatives & Animal Use in the Life Sciences*, **2007**, Special Issue, p. 397.
[41] T. Nann, *Nano Biomed. Eng.* **2011**, *3*, 137.
[42] Y. Yamamoto, N. Imai, R. Mashima, R. Konaka, M. Inoue, W. C. Dunlap, *Methods Enzymol.* **2000**, *319*, 29.
[43] F. Prat, R. Stackow, R. Bernstein, W. Qian, Y. Rubin, C. S. Foote, *J. Phys. Chem. A* **1999**, *103*, 7230.
[44] S. Wang, R. Gao, F. Zhou, M. Selke, *J. Mater. Chem.* **2004**, *14*, 487.
[45] J. A. Dahl, B. L. S. Maddux, J. E. Hutchison, *Chem. Rev.* **2007**, *107*, 2228.
[46] J. A. Riddick, W. B. Bunger, T. K. Sakano, *Organic solvents: physical properties and methods of purification*, New York, Wiley, **1986**.
[47] E. A. Almeida, S. Miyamoto, G. R. Martinez, M. H. G. Medeiros, P. D. Mascio, *Anal. Chim. Acta* **2003**, *482*, 99.

